

# Search for Gauge-Mediated Supersymmetry-Breaking Models using Diphoton Events with Missing Transverse Energy at CDF II

(Dated: June 23, 2009; Version 0.1; Line-count 510 out of 460)

We present the results of an optimized search for a gauge-mediated supersymmetry-breaking model where the lightest neutralino ( $\tilde{\chi}_1^0$ ) decays into a photon ( $\gamma$ ) and a gravitino producing  $\gamma\gamma$ +missing transverse energy events. In  $2.6\pm 0.2 \text{ fb}^{-1}$  of  $p\bar{p}$  collisions at  $\sqrt{s} = 1.96 \text{ TeV}$  recorded by the CDF II detector we observe no candidate events, consistent with a standard model background expectation of  $1.4\pm 0.4$  events. We set 95% C.L. cross section limits and place the world-best lower limit on the  $\tilde{\chi}_1^0$  mass ( $m_{\tilde{\chi}_1^0}$ ) of  $149 \text{ GeV}/c^2$  at a lifetime ( $\tau_{\tilde{\chi}_1^0}$ ) of  $\tau_{\tilde{\chi}_1^0} = 0 \text{ ns}$  as well as make exclusions in the  $m_{\tilde{\chi}_1^0-\tau_{\tilde{\chi}_1^0}}$  plane for  $\tau_{\tilde{\chi}_1^0} \lesssim 2 \text{ ns}$ .

PACS numbers: 13.85.Rm, 12.60.Jv, 13.85.Qk, 14.80.Ly

The standard model (SM) [1] of elementary particles has been enormously successful, but is incomplete. For theoretical reasons [2], and because of the observation of the ‘ $ee\gamma\gamma$ +missing transverse energy ( $\cancel{E}_T$ )’ [3, 4] candidate event by the CDF experiment during Run I at the Fermilab Tevatron, there is compelling rationale to search for the production and decay of new heavy particles that produce  $\gamma\gamma + \cancel{E}_T$  events in collider experiments. Of particular theoretical interest are supersymmetry (SUSY) models with gauge-mediated SUSY-breaking (GMSB) [2]. Since many versions of these models have a similar phenomenology we consider the scenario in which the lightest neutralino,  $\tilde{\chi}_1^0$ , decays almost exclusively into a photon and a weakly interacting, stable gravitino ( $\tilde{G}$ ) that gives rise to  $\cancel{E}_T$  by leaving a detector without depositing any energy [5]. The  $\tilde{G}$  is a warm dark matter candidate, favored in these models to have  $0.5 \text{ keV} < m_{\tilde{G}} < 1.5 \text{ keV}$  to be consistent with cosmological constraints [6]. Other direct searches [7–9] have constrained the mass of the  $\tilde{\chi}_1^0$  to have  $m_{\tilde{\chi}_1^0} \gtrsim 100 \text{ GeV}/c^2$  for much of the parameter space. Thus, at the Tevatron, sparticle production is dominated by gaugino pairs, and the  $\tilde{\chi}_1^0$  mass ( $m_{\tilde{\chi}_1^0}$ ) and lifetime ( $\tau_{\tilde{\chi}_1^0}$ ) are the two most important parameters in determining the final states and their kinematics. Complementary searches are required for  $\tau_{\tilde{\chi}_1^0} \gtrsim 1 \text{ ns}$  and  $\tau_{\tilde{\chi}_1^0} \lesssim 1 \text{ ns}$  [10].

In this letter we describe a search for GMSB models with  $\tau_{\tilde{\chi}_1^0} \leq 2 \text{ ns}$ , favored for large  $m_{\tilde{\chi}_1^0}$ , in which gaugino pairs are produced and decay to the  $\gamma\gamma + \cancel{E}_T + X$  final state where  $X$  are other high  $E_T$  final state particles. We use a dataset corresponding to an integrated luminosity of  $2.6\pm 0.2 \text{ fb}^{-1}$  of  $p\bar{p}$  collisions at  $\sqrt{s} = 1.96 \text{ TeV}$  from the Tevatron collected with the CDF II detector [11]. This work improves previous Tevatron searches [7, 8] for GMSB in this channel by using an upgraded detector with the EMTiming system [12], a larger data sample, and a new  $\cancel{E}_T$  Resolution Model (*Met Model*) [13]. The strategy is to select  $\gamma\gamma$  candidates and search for the presence of both significant  $\cancel{E}_T$  and large total event transverse energy to indicate the decays of heavy gauginos. We optimize the selection criteria based on the expected

sensitivity, taking into account the background and signal predictions.

A full description of the CDF Run II detector can be found elsewhere [11]. Here we briefly describe the aspects of the detector relevant to this analysis. The magnetic spectrometer consists of tracking devices inside a 3-m diameter, 5-m long superconducting solenoid magnet that operates at 1.4 T. A 3.1-m long drift chamber (COT) with 96 layers of sense wires is used to determine the momenta of charged particles, the  $z$  position of the  $p\bar{p}$  interaction, and the time of the interaction. The calorimeter, constructed of projective towers, each with an electromagnetic (EM) and hadronic (HAD) compartment, is divided into a central barrel that surrounds the solenoid coil ( $|\eta| < 1.1$ ) [3] and a pair of plug barrels that cover the region  $1.1 < |\eta| < 3.6$ . Both are used to identify photons, electrons, jets ( $j$ ) [14] and  $\cancel{E}_T$  and measure their 4-momenta. The EM calorimeters are instrumented with a timing system, EMTiming [12], that measures the arrival time of photons.

The analysis is performed in two stages, the creation of a  $\gamma\gamma$  event preselection sample with requirements to ensure events are well-measured [13], and then an optimization stage using kinematic requirements. We select candidate events using both online (during data taking) and offline selection requirements. Online, events are selected by the three-level trigger as passing one of four triggers [13] that, when combined, are effectively 100% efficient for our diphoton events where both photons have  $|\eta| < 1.1$  and  $E_T > 13 \text{ GeV}$ . Offline, both photons are required to be in the fiducial part of the calorimeter and pass the standard photon identification and isolation requirements [7] with two minor modifications to remove instrumental and electron backgrounds [13, 15].

This set of events is dominated by SM production of  $\gamma\gamma, \gamma j$  with  $j \rightarrow \gamma_{fake}$  and  $jj \rightarrow \gamma_{fake}\gamma_{fake}$ , but there are also electroweak sources with real  $\cancel{E}_T$  and non-collision backgrounds. To minimize the number of SM events in the presample with large  $\cancel{E}_T$  due to calorimeter energy mismeasurement we remove events if the  $\cancel{E}_T$  vector points along the direction, within  $|\Delta\phi| < 0.3$ , of the second photon or a narrow jet, with  $E_T^j > 5 \text{ GeV}$  and  $|\eta| < 2.5$ ,

located close to the calorimeter cracks at  $\eta \sim 0$  and  $|\eta| \sim 56$  1.1 where these objects can be partially lost [13]. To 57 help maintain the projective nature of the calorimeter 58 we require a vertex with  $|z_{\text{vertex}}| < 60$  cm, which also 59 helps to reduce non-collision backgrounds. For events 60 with multiple reconstructed vertices we pick the vertex 61 with the highest  $\sum_{\text{tracks}} p_T$  [3], except when if assigning 62 the photons to a different vertex lowers the  $\cancel{E}_T$ , we take 63 that  $\cancel{E}_T$  and the photon  $E_T$ 's to be from that vertex for 64 all calculations. 65

Non-collision backgrounds coming from cosmic ray and 66 beam-related effects can produce diphoton candidates 67 and  $\cancel{E}_T$ , and are removed from the presample using a 68 number of techniques. Photon candidates from cosmic 69 rays are not correlated in time with collisions. We reject 70 events if the photon time of arrival at the calorimeter, 71 corrected for average path length ( $t_\gamma$ ) has  $t_\gamma > 4\sigma_t$  or 72  $|t_{\gamma 1} - t_{\gamma 2}| > 4\sigma_{|t_1 - t_2|}$ , where  $\sigma_t = 1.66$  ns and is a mea- 73 surement of consistency with being from the collision and 74  $\sigma_{|t_1 - t_2|} = 1.02$  ns. Photon candidates can also be pro- 75 duced by beam-related muons that originate upstream 76 of the detector (mostly from the more intense  $p$  beam) 77 and travel through the calorimeter, typically depositing 78 small amounts of energy near  $\phi \approx 0$  for geometrical rea- 79 sons. These are suppressed using standard beam halo 80 (BH) identification requirements [15]. A total of 38,053 81 diphoton candidate events pass the preselection require- 82 ments. 83

Backgrounds to the  $\gamma\gamma + \cancel{E}_T$  final state come from SM 84 production where  $\cancel{E}_T$  arises due to energy mismeasure- 85 ments in the calorimeter or event reconstruction patholo- 86 gies. To select events with real and significant  $\cancel{E}_T$ , as 87 part of the optimization, and to predict the contribution 88 of SM backgrounds with mismeasured (“fake”)  $\cancel{E}_T$  due to 89 normal energy measurement fluctuations, we use a *Met* 90 *Model* [13]. This model considers the clustered (jets) and 91 unclustered energy in the event and calculates a proba- 92 bility for fluctuations in the energy measurement to pro- 93 duce  $\cancel{E}_T^{\text{fluct}}$  equivalent to or larger than the measured 94  $\cancel{E}_T$  ( $P_{\cancel{E}_T^{\text{fluct}} > \cancel{E}_T}$ ). This probability is then used to define 95 a  $\cancel{E}_T$ -significance as  $-\log_{10} \left( P_{\cancel{E}_T^{\text{fluct}} > \cancel{E}_T} \right)$ . Events with 96 true and fake  $\cancel{E}_T$  of the same value should have, on aver- 97 age, different  $\cancel{E}_T$ -significance. To estimate the expected 98  $\cancel{E}_T$ -significance distribution for SM events with fake  $\cancel{E}_T$ , 99 and the number of mismeasured events above a given  $\cancel{E}_T$ , 100 significance requirement, we use a pseudo-experiments 101 method where we smear the jets and unclustered energy, 102 using appropriate resolutions in the event. The system- 103 atic uncertainty is evaluated by comparing the *Met Model* 104 predictions with a default set of parameters to predic- 105 tions obtained with parameters varied by one standard 106 deviation. Statistical uncertainties are added in quadra- 107 ture with the systematic uncertainties to obtain the total 108 uncertainty. 109

Event reconstruction pathologies in SM events with no 110

intrinsic  $\cancel{E}_T$ , such as a wrong choice of the primary inter- action vertex or tri-photon events with a lost photon, are unaccounted for by the *Met Model*. To obtain the pre- diction for this background we model SM kinematics and event reconstruction using a PYTHIA [16]  $\gamma\gamma$  sample with a detector simulation [17] and normalize to the number of events in the presample to take into account  $\gamma j$  and  $j j$  contributions to the backgrounds. We subtract off the expectations for energy mismeasurement fluctuations in the MC to avoid double counting. The systematic uncer- tainties on this background prediction includes the un- certainty due to MC-data differences in the unclustered energy parameterization and on the jet energy scale.

Electroweak production of  $W$ 's and  $Z$ 's which decay to leptons can also give rise to the  $\gamma\gamma + \cancel{E}_T$  signature where one or more of the photons can be fake, but the  $\cancel{E}_T$  is due to one or more neutrinos. To estimate the contribution from these backgrounds we use MC simulations [17], nor- malized to their production cross sections and consider- ing all the leptonic decay modes of the bosons. The Baur MC [18] is used to simulate  $W\gamma$  and  $Z\gamma$  production and decay where initial and final state radiation (ISR/FSR) simulates  $W/Z + \gamma\gamma$  events. The PYTHIA [16] MC is used to simulate  $W$ ,  $Z$ , with photons from ISR/FSR removed, and  $t\bar{t}$  backgrounds where both photon candidates are fakes. To minimize the dependence of our predictions on potential Data-MC differences we scale our MC produc- tions to the observed number of  $e\gamma$  events in data where we use the same diphoton triggers and analysis selection procedures as used for our  $\gamma\gamma$  sample. Uncertainties are dominated by the  $e\gamma$  normalization uncertainty.

Non-collision backgrounds are estimated using the data. Using the sample selection requirements, but re- quiring one of the photons to have  $t_\gamma > 25$  ns we iden- tify a cosmic enhanced sample. Similarly, we select a beam related background enhanced sample. Using ex- trapolation techniques and the measured efficiencies of the non-collision rejection requirements we estimate the number of these events in the signal region [13]. The un- certainties on both non-collision background estimates are dominated by statistical uncertainty on the number of identified events. The  $\cancel{E}_T$ -significance distribution for the presample, along with shape of the predictions for all the backgrounds, is shown in Figure 1.

We estimate the sensitivity to heavy, neutral parti- cles that decay to photons using the GMSB reference model [5] in the mass-lifetime range,  $75 \leq m_{\tilde{\chi}_1^0} \leq 150$  GeV and  $\tau_{\tilde{\chi}_1^0} \leq 2$  ns. Events from all SUSY pro- cesses are simulated with PYTHIA [16] and a detector simulation [17]. The acceptance, used in the optimization procedure and limit setting, is taken to be equal to the ratio of simulated events that pass all the requirements to all events produced. The acceptance is a strong function of the fraction of  $\tilde{\chi}_1^0$  decays that occur in the detector volume, which is dependent on both  $\tau_{\tilde{\chi}_1^0}$  and the masses

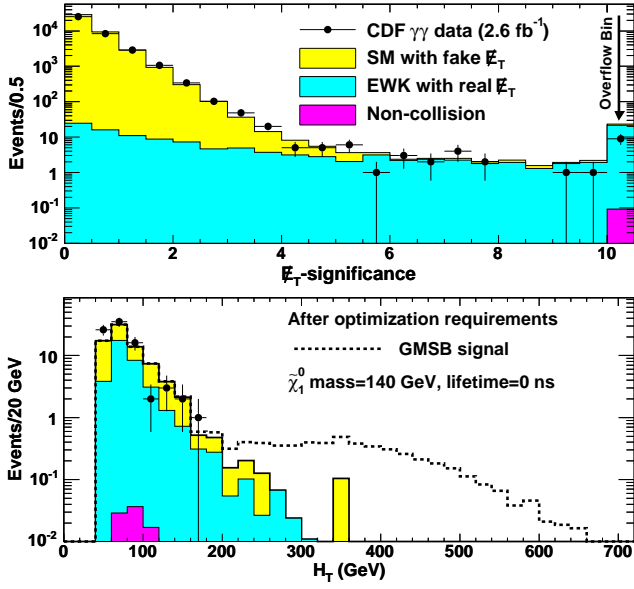


FIG. 1: The top plot shows the expected background  $E_T$ -significance prediction for the  $\gamma\gamma$  candidate sample, along with the data, after the preselection requirements. The bottom plot shows the predicted  $H_T$  distribution after all but the optimized  $H_T$  requirement. There is no evidence for new physics and the data is well modeled by backgrounds alone.

of the particles, all of which scale linearly with  $m_{\tilde{\chi}_1^0}$  for our model [10]. The total systematic uncertainty on the acceptance, after all kinematic requirements, is estimated to be 7%, dominated by the uncertainty on the photon ID efficiency (2.5% per photon). Other significant contributions come from uncertainties on ISR/FSR (4%), jet energy measurement (2%),  $E_T$ -significance parameterizations (1%) and the parton distribution functions (1%).

We determine the kinematic selection requirements that define the final data sample by optimizing the mean expected 95% confidence level (C.L.) cross section limit in the no-signal assumption without looking at the data in the signal region [19]. To compute the predicted cross section upper limit we combine the luminosity, the acceptance and the background estimates with the systematic uncertainties using a Bayesian method [20]. The predicted limits are optimized by simultaneously varying the selection requirements for  $E_T$ -significance,  $H_T$  (total  $E_T$  of photons, jets and  $E_T$ ), and the azimuthal angle between the two leading photons,  $\Delta\phi(\gamma_1, \gamma_2)$ . The large  $E_T$ -significance requirement gets rid of most of the SM background with fake  $E_T$ . GMSB production is dominated by heavy gaugino pairs which decays to high  $E_T$ , light final state particles via cascade decays. GMSB signal has, on average, larger  $H_T$  compared to SM backgrounds so that an  $H_T$  requirement can remove these backgrounds effectively. Electroweak backgrounds with large  $H_T$  are typically a high  $E_T$  photon recoiling against

$W \rightarrow e\nu \rightarrow \gamma_{fake} E_T$ , which means the gauge boson decay is highly boosted. Thus, the two photon candidates in the final state are mostly back to back. Also, the high  $E_T$  diphotons with large  $H_T$  from SM background are mostly back-to-back with fake  $E_T$ ; the  $\Delta\phi(\gamma_1, \gamma_2)$  cut reduces both these backgrounds.

While each point in the considered  $\tau_{\tilde{\chi}_1^0}$  vs.  $m_{\tilde{\chi}_1^0}$  space gives a slightly different optimization, we choose a single set of requirements because it maximizes the expected 95% C.L. exclusion region; where the predicted production cross section at next-to-leading order [21] is above the expected cross section limit. The exclusion region also takes into account the production cross section uncertainties which are dominated by the parton distribution functions (7%) and the renormalization scale (3%). We find the optimal set of cuts, before unblinding the signal region, to be:  $E_T$ -significance  $> 3$ ,  $H_T > 200$  GeV, and  $\Delta\phi(\gamma_1, \gamma_2) < \pi - 0.35$  rad. With these requirements we predict  $1.38 \pm 0.44$  background events with real  $E_T$ ,  $0.46 \pm 0.24$  from SM with fake  $E_T$ , and  $0.001^{+0.008}_{-0.001}$  from non-collision.

No events in the data pass the final event selection. The acceptance for  $m_{\tilde{\chi}_1^0} = 140$  GeV/ $c^2$  and  $\tau_{\tilde{\chi}_1^0} = 0$  ns is estimated to be  $7.8 \pm 0.6\%$  and the  $H_T$  distribution, normalized to expectations, is shown in Figure 1, after all but the final  $H_T$  cut. Since the data is consistent with the no-signal hypothesis, we set cross section limits as a function of  $m_{\tilde{\chi}_1^0}$  and  $\tau_{\tilde{\chi}_1^0}$  respectively, as shown in Figure 2. The  $m_{\tilde{\chi}_1^0}$  reach, based on the predicted and observed number of events for  $\tau_{\tilde{\chi}_1^0} = 0$ , is 141 GeV/ $c^2$  and 149 GeV/ $c^2$  respectively. These limits significantly extend the search sensitivity beyond the results of D0 [8] and, when combined with the complementary exclusions from CDF and LEP [9, 15], cover the region shown in Figure 3.

In conclusion, we have performed an optimized search for heavy, neutral particles that decay to photons in the  $\gamma\gamma + E_T$  final state using 2.6 fb $^{-1}$  of data. There is no excess of events beyond expectations. We set cross section limits using a GMSB model with  $\tilde{\chi}_1^0 \rightarrow \gamma\tilde{G}$ , and find an exclusion region in the  $\tau_{\tilde{\chi}_1^0}$ - $m_{\tilde{\chi}_1^0}$  plane with a world-best 95% C.L. lower limit on the  $\tilde{\chi}_1^0$  mass of 149 GeV/ $c^2$  at  $\tau_{\tilde{\chi}_1^0} = 0$  ns. By the end of Run II, an integrated luminosity of 10 fb $^{-1}$  is possible for which we estimate a mass reach of  $\simeq 160$  GeV/ $c^2$  at a lifetime of 0 ns by scaling the expected number of background events.

We thank the Fermilab staff and the technical staffs of the participating institutions for their vital contributions. This work was supported by the U.S. Department of Energy and National Science Foundation; the Italian Istituto Nazionale di Fisica Nucleare; the Ministry of Education, Culture, Sports, Science and Technology of Japan; the Natural Sciences and Engineering Research Council of Canada; the National Science Council of the

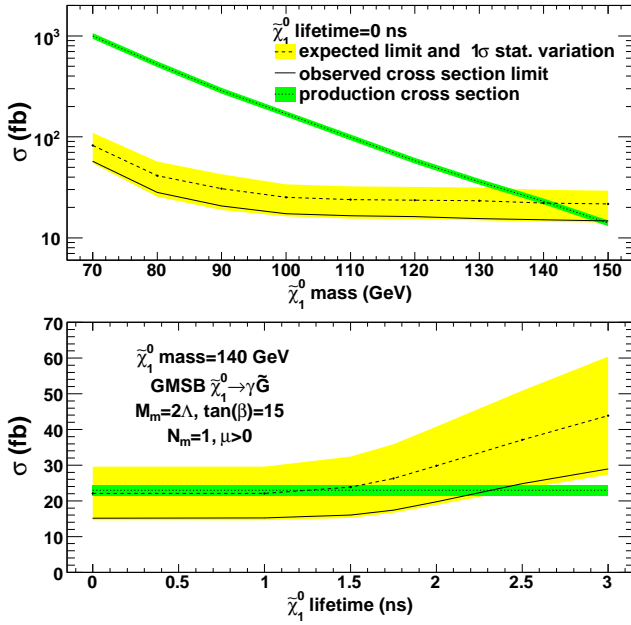


FIG. 2: The predicted and observed 95% C.L. cross section upper limits as a function of the  $\tilde{\chi}_1^0$  mass at a lifetime of 0 ns (top) and as a function of the  $\tilde{\chi}_1^0$  lifetime at a mass of 140 GeV/c<sup>2</sup> (bottom). Indicated in green (darker shading) is the production cross section, along with its 8.0% uncertainty-band. In yellow (lighter shading) is the RMS variation on the expected cross section limit.

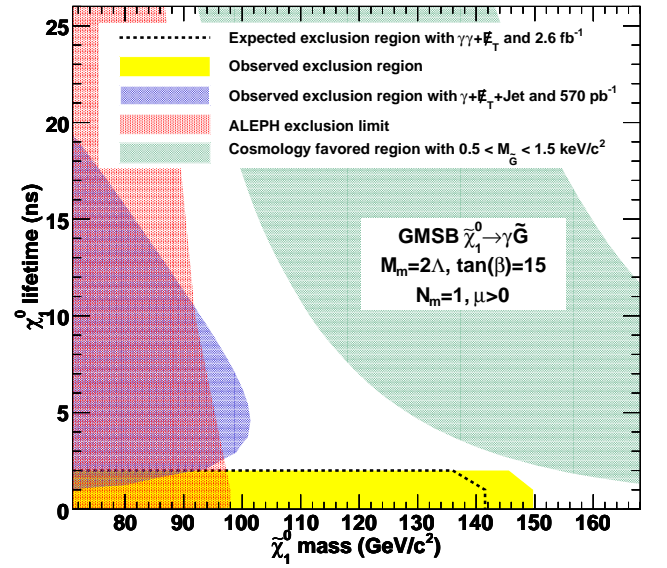


FIG. 3: The predicted and observed exclusion region along with the limit from ALEPH/LEP [9] and the CDF  $\gamma + \cancel{E}_T + jet$  ‘delayed’ photon analysis [15]. We have a mass reach of 141 GeV/c<sup>2</sup> (predicted) and 149 GeV/c<sup>2</sup> (observed) at lifetimes up to 1 ns. The shaded band shows the parameter space where  $0.5 < m_{\tilde{G}} < 1.5$  keV/c<sup>2</sup>, favored in cosmologically consistent models [6].

Republic of China; the Swiss National Science Foundation; the A.P. Sloan Foundation; the Bundesministerium für Bildung und Forschung, Germany; the Korean Science and Engineering Foundation and the Korean Research Foundation; the Particle Physics and Astronomy Research Council and the Royal Society, UK; the Russian Foundation for Basic Research; the Comisión Interministerial de Ciencia y Tecnología, Spain; in part by the European Community’s Human Potential Programme under contract HPRN-CT-2002-00292; and the Academy of Finland.

- [1] See for example, F. Halzen and A. D. Martin, *Quarks and Leptons* (John Wiley & Sons, New York, 1984); C. Quigg, *Gauge Theories of the Strong, Weak, and Electromagnetic Interactions* (Addison-Wesley, Reading, MA, 1983); I. S. Hughes, *Elementary particles* (Cambridge University Press, Cambridge, England, 1990).
- [2] S. Dimopoulos, S. Thomas, J. D. Wells, Nucl. Phys. B **488**, 39 (1997); S. Ambrosanio, G.D. Kribs and S.P. Martin, Phys. Rev. D **56**, 1761 (1997); G. F. Giudice and R. Rattazzi, Phys. Rept. **322**, 419 (1999); and S. Ambrosanio, G. Kane, G. Kribs, S. Martin and S. Mrenna, Phys. Rev. D **55**, 1372 (1997).
- [3] We use a cylindrical coordinate system in which the proton beam travels along the  $z$ -axis,  $\theta$  is the polar angle,  $\phi$  is the azimuthal angle, and  $\eta = -\ln \tan(\theta/2)$ . The transverse energy and momentum are defined as  $E_T = E \sin \theta$  and  $p_T = p \sin \theta$  where  $E$  is the energy measured by the calorimeter and  $p$  the momentum measured in the tracking system.  $\cancel{E}_T = |-\sum_i E_T^i \vec{n}_i|$  where  $\vec{n}_i$  is a unit vector that points from the interaction vertex to the  $i$ th calorimeter tower in the transverse plane.

- [4] F. Abe *et al.* (CDF Collaboration), Phys. Rev. Lett. **81**, 1791 (1998) and Phys. Rev. Lett. **59**, 092002 (1999).
- [5] B. C. Allanach *et al.*, Eur. Phys. J. C **25**, 113 (2002). We use benchmark model 8 and take the messenger mass scale  $M_{\text{mess}} = 2\Lambda$ ,  $\tan(\beta) = 15$ ,  $\mu > 0$  and the number of messenger fields  $N_{\text{mess}} = 1$ . The  $\tilde{G}$  mass factor and the supersymmetry breaking scale  $\Lambda$  are allowed to vary independently.
- [6] C.-H. Chen and J. F. Gunion, Phys. Rev. D **58**, 075005 (1998).
- [7] D. Acosta *et al.* (CDF Collaboration), Phys. Rev. D **71**, 031104 (2005).
- [8] V.M. Abazov *et al.* (D0 Collaboration), Phys. Lett. B **659**, 856 (2008).
- [9] A. Heister *et al.* (ALEPH Collaboration), Eur. Phys. J. C **25**, 339 (2002); also see M. Gataullin, S. Rosier, L. Xia and H. Yang, arXiv:hep-ex/0611010; G. Abbiendi *et al.* (OPAL Collaboration), Proc. Sci. HEP2005 346 (2006); J. Abdallah *et al.* (DELPHI Collaboration), Eur. Phys. J. C **38** 395 (2005).
- [10] D. Toback and P. Wagner, Phys. Rev. D **70**, 114032 (2004).
- [11] D. Acosta *et al.* (CDF Collaboration), Phys. Rev. D **71**, 032001 (2005).
- [12] M. Goncharov *et al.*, Nucl. Instrum. Methods A **565**, 543 (2006).

- [13] R. Culbertson, A. Pronko, S. Yu, M. Goncharov,  $\gamma\gamma + X$  PRD in progress.
- [14] For a description of how clusters of energy, for example  $\tau^\pm \rightarrow \pi^\pm \pi^\mp \pi^\pm \nu_\tau$  decays, are identified as jets, see F. Abe *et al.* (CDF Collaboration), Phys. Rev. Lett. **68** (1104) 1992. For a discussion of the jet energy measurements, see T. Affolder *et al.* (CDF Collaboration), Phys. Rev. D **64** (032001) 2001. For a discussion of standard jet correction systematics, see A. Bhatti *et al.*, Nucl. Instrum. Methods, A 566, 375 (2006). We use jets with cone size  $\Delta R = 0.4$ .
- [15] A. Abulencia *et al.* (CDF Collaboration), Phys. Rev. Lett. **99**, 121801 (2007); T. Aaltonen *et al.* (CDF Collaboration), Phys. Rev. D **78**, 032015 (2008).
- [16] T. Sjöstrand *et al.*, Comput. Phys. Commun. **135**, 238 (2001). We use version 6.216.
- [17] We use the standard GEANT based detector simulation [R. Brun *et al.*, CERN-DD/EE/84-1 (1987)] and add a parametrized EMTiming simulation.
- [18] U. Baur, T Han and J. Ohnemus, Phys. Rev. D **48**, 5140 (1993); U. Baur, T Han and J. Ohnemus, Phys. Rev. D **57**, 2823 (1998); The  $W\gamma$  and  $Z\gamma$  processes are simulated using the leading-order event generator and have a k-factor fixed at 1.36. The initial and final state radiations (resulting in additional jets or photons), underlying event, and additional interactions are simulated by the PYTHIA Monte Carlo program [16].
- [19] E. Boos, A. Vologdin, D. Toback, and J. Gaspard, Phys. Rev. D **66**, 013011 (2002).
- [20] J. Conway, CERN Yellow Book Report No. CERN 2000-005, 2000, p. 247. We assume a flat prior in the production cross section.
- [21] We use the leading-order cross sections generated by the PYTHIA [16] event generator and use the k-factors produced by PROSPINO 2.0 [W. Beenakker *et al.*, Phys. Rev. Lett. **83**, 3780 (1999)].